Trimer Liquids and Crystals of Polar Molecules in Coupled Wires

M. Dalmonte,[1,2] P. Zoller,[2] and G. Pupillo[2,3]

[1]*Dipartimento di Fisica dell'Università di Bologna and INFN, via Irnerio 46, 40127 Bologna, Italy*
[2]*IQOQI and Institute for Theoretical Physics, University of Innsbruck, A-6020 Innsbruck, Austria*
[3]*ISIS (UMR 7006) and IPCMS (UMR 7504), Université de Strasbourg and CNRS, Strasbourg, France*

(Received 22 March 2011; published 11 October 2011)

We investigate pairing and crystalline instabilities of bosonic and fermionic polar molecules confined to a ladder geometry. Combining analytical and numerical techniques, we show that gases of composite molecular dimers as well as trimers can be stabilized as a function of the density difference between the wires. A shallow optical lattice can pin both liquids, realizing crystals of composite bosons and fermions. We show that these exotic quantum phases are robust against conditions of confinement of the molecular gas to harmonic finite-size potentials.

DOI: 10.1103/PhysRevLett.107.163202 PACS numbers: 34.20.−b, 03.75.Lm, 05.30.Jp, 71.10.Pm

Binding among three or more particles plays a fundamental role in various physical systems ranging from quark confinement in QCD to tetramer biexciton formation in carbon nanotubes [1]; in quantum magnets, it is responsible for the formation of many-body quantum phases of spin multipoles [2]. In atomic quantum gases, two-body pairing is at the heart of paradigmatic phenomena, such as the observation of the Bose-Einstein condensation-BCS crossover [3] in mixtures of ultracold fermionic atoms and the prediction of Fulde-Ferrell-Larkin-Ovchinnikov [4] and Sarma [5] phases in spin-unbalanced gases. The study of few-body pairing, however, is usually confined to Efimov-like resonances [6], while the realization of finite-density liquids made of composite particles is hindered by losses due to three-body recombination. Polar molecules confined to low-dimensional geometry provide a new opportunity to study intermolecular pairing mechanisms and the associated quantum phases in a setup where collisional losses and also chemical reactions are suppressed [7–9]. Pairing of two spin-polarized fermionic molecules across coupled two-dimensional (2D) layers [10] or one-dimensional (1D) wires [11] has already lead to the prediction of, e.g., 2D interlayer superfluidity [12] for the special case where the number of molecules is the same in all layers (wires). However, the pairing dynamics in the general situation where this number can vary across the layers (wires), as it happens in experiments [8], has so far remained largely unexplored. Different particle numbers in the layers lower the overall (spin-rotational) symmetry of the problem, which makes the underlying physics drastically different [13]: A general pairing mechanism may exist for the formation of stable multimolecule composite structures. The goal is now to determine whether (spin-rotational) symmetry breaking induces stable multimer liquids in confined quantum gases, where few-body processes are usually associated with resonances and losses [6].

In this Letter, we study a situation where polar molecules are confined to two coupled 1D wires, under conditions where the number of molecules can be the same or vary across the wires, similar to current experiments. This presents several new scenarios: (i) When the population is identical in the wires, a two-body bound state is always present and is responsible for the appearance of dimer liquids, similar to 2D [12]; see Fig. 1(c). However, we find that (ii) *few-body* pairing is favored for *any* ratio of populations between the wires $P = p/q$, with $p, q \in \mathbb{N}$, which is a dense set between $]0, 1]$. This leads to the stabilization of novel quantum phases of interacting

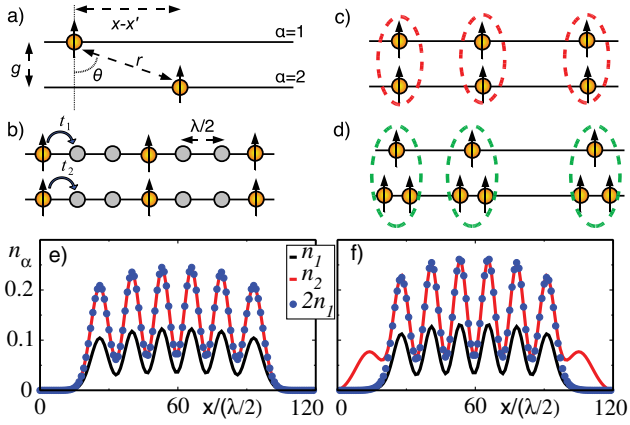

FIG. 1 (color online). (a) Molecules with dipole strength d_α ($\alpha = 1, 2$) in a two-leg ladder with interwire distance g and dipolar interactions $V(r) = d_1 d_2 (1–3\cos^2\theta)/r^3$. (b)–(d) Sketch of phases (see the text): (b) dimer crystal in a lattice with spacing $\lambda/2$ and hopping energy t_α; (c) dimer liquid; (d) trimer liquid. (e)–(f) Numerical results for density distributions n_α vs position x in the presence of an optical lattice along the wires [see (b)] and weak harmonic confinement, showing trimers. Parameters [see also Eq. (1) and the text]: $g = \lambda/2$, hopping asymmetry $t_2/t_1 = 0.01$, $d_1/d_0 = 3$, $d_2/d_0 = 0.5$ with $d_0^2 = t_1 g^3$; the curvature of the harmonic potential is $\mathcal{K}/t_1 = 0.03$ (see the text). Particle numbers N_α: (e) $N_2 = 2N_1 = 12$; (f) $N_2 = 2N_1 + 2 = 14$; as a reference, blue points denote $2n_1$. The trap center is at $x/(\lambda/2) = 60$.

fermionic or bosonic composite particles, where repulsive intrawire interactions ensure collisional stability. In particular, we prove that a gas of trimers made of two particles on one wire and one in the other may be stabilized in these systems [Fig. 1(d)]. Both dimer and trimer liquids may be pinned by a weak period potential commensurate with the density, leading to a Luttinger staircase of quasi-1D composite crystals [14]. By numerical simulations, we show that these exotic quantum phases are robust to conditions of trapping in parabolic finite-size potentials and number fluctuations in the wires: Unusual ''wedding-cake'' structures are formed where heavy composite particles are flanked by lighter ones [Figs. 1(e) and 1(f)].

Our starting point is the Hamiltonian $H = \sum_\alpha H_\alpha + H_{12}$ for the dynamics of molecules in the configuration of Fig. 1, with $\alpha = 1, 2$, H_α the single-wire term

$$H_\alpha = \int dx \psi_\alpha^\dagger(x)\left[-\frac{\hbar^2}{2m_\alpha}\partial_x^2 + U_\alpha(x)\right]\psi_\alpha(x) + \frac{d_\alpha^2}{8\pi}\int dx dx' \frac{1}{|x-x'|^3} n_\alpha(x) n_\alpha(x'), \quad (1)$$

and $H_{12} = (d_1 d_2)/(8\pi)\int dx dx' V(x-x') n_1(x) n_2(x')$ the interwire coupling, with $V(x-x') = [1\text{–}3\cos^2(\theta)]/[g^2 + (x-x')^2]^{3/2}$ showing a short-distance interwire attraction. Here, m_α and d_α are the mass and the dipole strength, respectively, and ψ_α ($\psi_\alpha^\dagger$) are fermionic or bosonic annihilation (creation) operators, with $n_\alpha(x) = \psi_\alpha^\dagger(x)\psi_\alpha(x)$; $U_\alpha(x) = \mathcal{U}_\alpha \sin^2(2\pi x/\lambda)$ represents an underlying periodic potential, as usually provided by an optical lattice [15] with wavelength λ and depth $\mathcal{U}_\alpha$; θ is the angle between particles in different wires, with distance g (Fig. 1). The 1D Hamiltonian H is valid for interparticle distances $n_\alpha^{-1} \gg (d_\alpha^2/\hbar\omega_\perp)^{1/3}$ with $\omega_\perp$ the frequency of transverse confinement provided by, e.g., a 2D optical lattice. For LiCs, RbCs, and KRb molecules with $d_1 =$ 5.6, 1.25, and 0.5 Debye, respectively, and $\omega_\perp = 2\pi \times$ 100 kHz, $(d_\alpha^2/\hbar\omega_\perp)^{1/3}$ is of the order of 360, 130, and 70 nm, respectively [7]. In addition, $d_1 d_2/g^3 < \mathcal{U}_\alpha$ [16]. Similar setups may be obtained on chip-based microtraps [17].

In Ref. [14], it is shown that, in the absence of an optical lattice ($U_\alpha = 0$) and of interwire interactions, the dynamics in each wire is described by an effective Tomonaga-Luttinger liquid (TLL) theory with Hamiltonian [18]

$$\mathcal{H}_\alpha = \frac{\hbar v_\alpha}{2\pi}\int dx\{[\partial_x\vartheta_\alpha(x)]^2/K_\alpha + K_\alpha[\partial_x\phi_\alpha(x)]^2\}.$$

Here v_α and $K_\alpha = (1 + 0.73 n_\alpha R_\alpha)^{-1/2}$ are the effective sound velocity and the TLL parameter, respectively [14], with $R_\alpha = m_\alpha d_\alpha^2/(2\pi\hbar^2)$ the intrawire dipole length, and ϑ_α and ϕ_α represent long-wavelength density and phase fluctuations, respectively [18]. For finite interactions, Eq. (1) is then effectively described by $\mathcal{H} = \sum_\alpha \mathcal{H}_\alpha + \mathcal{H}_{12}$, with $\mathcal{H}_{12} = \mathcal{H}_f + \mathcal{H}_b$. Here, in the weak coupling regime we obtain $\mathcal{H}_f = -\frac{d_1 d_2}{24 g^2 \pi^3}\int dx \partial_x\vartheta_1(x)\partial_x\vartheta_2(x)$ for the *quadratic* forward-scattering part of the interactions [18], by approximating the interwire interaction with its zero-component Fourier transform[18]; $\mathcal{H}_b$ is the *backscattering* part, with a typical sine-Gordon-type form, to be discussed below. The effect of $\mathcal{H}_f$ is to modify the effective TLL parameters, while $\mathcal{H}_b$ can induce novel pairing instabilities. Here, we first discuss the case of two identical (*balanced*) coupled wires and then the more general case of (*unbalanced*) wires with different densities, molecular masses, and interactions.

In the balanced case, the quadratic part $\sum_\alpha \mathcal{H}_\alpha + \mathcal{H}_f$ of $\mathcal{H}$ can be diagonalized by introducing standard charge and spin fields, $\vartheta_{c,s} = (\vartheta_1 \pm \vartheta_2)/\sqrt{2}$ [19], leading to a description in terms of coupled TLLs with effective parameters $K_{c,s}$. For weak interactions we estimate $K_{c,s} = K_1[1 \mp \Gamma_{12} K_1/v_1]^{-1/2}$, $\Gamma_{12} = d_1^2/(24\pi^2\hbar g^2)$. The term $\mathcal{H}_b$ has the sine-Gordon-type form $\mathcal{H}_b \propto -\frac{n_1^2 d_1 d_2}{12 g^2 \pi}\int dx \cos[2\sqrt{2}\vartheta_s(x)]$, and, in agreement with Berezinskii-Kosterlitz-Thouless theory [18,20], it is relevant, thus opening a spin gap (e.g., pairing), if $K_s < 1$; this condition is always satisfied and shows that, similar to the 2D case, pairing of molecules across the wires is always favored in 1D, even for an infinitesimally small attraction between the wires with g, $R_\alpha \ll n_\alpha^{-1}$. The role of dipolar interactions is evident in the charge sector: In contrast to models with attractive contact interactions such as the Hubbard model [18], here K_c can be much smaller than 1; as an example, in the strongly interacting regime $n_\alpha R_\alpha \gg 1$, where dimers are well approximated by tightly bound composite particles with effective mass $M = 2m$ and dipole strength $D = 2d$, $K_c \simeq 2/(1 + 5.8 n_\alpha R_\alpha)^{1/2}$. As a result, the many-body ground state shows a crossover from a dimer liquid (DL) with dominant pair correlations $\mathcal{D}(x) = \langle \psi_{1,i}^\dagger \psi_{2,i}^\dagger \psi_{1,i+x}\psi_{2,i+x}\rangle \sim |x|^{-1/K_c}$ for $K_c > 1$ to a charge-density wave (CDW) with dominant density correlations $\mathcal{G}(x) = \langle n_i n_{i+x}\rangle \sim |x|^{-K_c}$ for $K_c < 1$, $n_i = n_{i,1} + n_{i,2}$. In this regime, the CDW can be pinned by a very shallow optical lattice commensurate with the particle density, stabilizing a Luttinger staircase [14] of dimer crystals (see [19] for more details).

We verify numerically these predictions in the deep lattice regime $\mathcal{U}/E_r \gg 1$, with E_r the lattice recoil, where an appropriate description is given in terms of an anisotropic extended Hubbard model [21]:

$$\hat{H} = -\sum_{\alpha,i} t_\alpha (c_{\alpha,i}^\dagger c_{\alpha,i+1} + \text{H.c.}) - \frac{2 d_1 d_2}{g^3}\sum_i n_{1,i} n_{2,i} + \sum_{i<j}\left[d_1 d_2 V_{ij}(n_{1,i} n_{2,j} + n_{2,i} n_{1,j}) + \sum_\alpha \frac{d_\alpha^2 n_{\alpha,i} n_{\alpha,j}}{(j-i)^3}\right],$$

which we analyze by using a quasi-exact density-matrix-renormalization-group technique [22]. Here, V_{ij} describes the anisotropic part of the dipolar interaction, and $t_\alpha = 1$

sets the energy scale. In the balanced case, $d_\alpha = d$ and $n_\alpha = n$. The field theoretical description of the anisotropic extended Hubbard model in terms of continuum fields is equivalent to the one in the limit of a shallow lattice given above, and we thus expect a similar qualitative behavior.

Figure 2 shows the phase diagram for a commensurate density $n_\alpha = 0.2$. By fixing $g = \lambda/4$ and increasing d, we find first a crossover from a TLL of dimers (DL) to a CDW and then a Berezinskii-Kosterlitz-Thouless–type pinning quantum phase transition to a dimer crystal (DC) with $n_\alpha = 1/5$ (phase boundaries are discussed in Ref. [19]). Examples of $\mathcal{D}(x)$ are plotted in Fig. 2(b) for all three phases, where the dash-dotted line marks the transition from power-law to exponential decay. We also calculate the spin gap Δ_s, by performing a finite-size scaling of $\Delta_s(L) = E_L(N, N) - E_L(N+1, N-1)$, with $E_L(M, M')$ the ground state energy at finite size L in the sector with $n_1 = M$, $n_2 = M'$, for different densities and g [inset in Fig. 2(a)]. We find that a finite gap is present in the entire phase diagram, as expected, although it is small for weak interactions due to the Berezinskii-Kosterlitz-Thouless scaling $\Delta_s \propto \exp[-\beta d^2]$ [18].

The unbalanced case presents unconventional instabilities. As shown in Ref. [13], the Haldane expansion of density operators in a two-component TLL generates an infinite series of massive terms coming from different combinations of vertex operators

$$\mathcal{H}_b = \sum_{p,q\in\mathbb{N}} G_{p,q} \int dx \cos[2x(pk_{F1} - qk_{F2}) + 2(p\theta_1 - q\theta_2)],$$

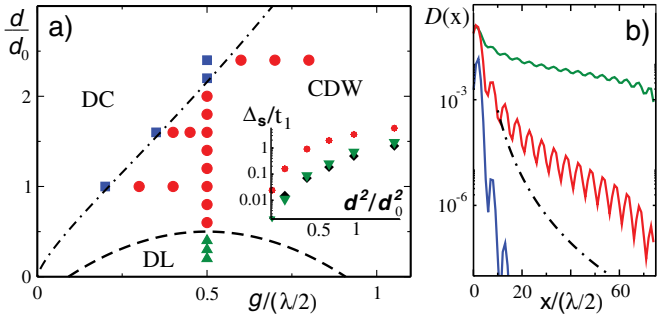

FIG. 2 (color online). (a) Phase diagram in the balanced case with $d_\alpha = d$, $t_2 = t_1$, and $n_\alpha = 0.2$ on a lattice with spacing $\lambda/2$ and $d_0^2 = t_1(\lambda/2)^3$. Green triangles, red circles, and blue squares are numerical results for DL, CDW, and DC phases, respectively; dashed and dashed-dotted lines are qualitative phase boundaries. Inset: Scaling of the dimer-pairing spin gap Δ_s as a function of d^2 for several example densities n_α and interwire distances g: [$n_\alpha = 0.2$, $g = 0.35\lambda$] (red points), [0.4, $\lambda/2$] (green triangles), and [0.2, $\lambda/2$] (black diamonds). (b) Dimer correlation function $\mathcal{D}(x)$ vs x in the phases of (a), with $g/(\lambda/2) = 0.5$, $n_\alpha = 0.2$. Top to bottom (continuous lines): $d/d_0 = 0.5$ (DL), 1.3 (CDW), and 2.2 (DC); the dashed-dotted line is the CDW-DC quantum phase transition at $\sim x^{-25/4}$.

where $G_{p,q}$ are model-dependent coefficients and $k_{F\alpha} = \pi n_\alpha$. With the exception of the simplest case $p = q = 1$, these terms are usually negligible from a renormalization group point of view. However, we find that strong dipolar interactions drastically enhance the effect of $\mathcal{H}_b$ [19], allowing the formation of *multiparticle composites* [13], or multimers, made of p (q) particles on the upper (lower) wire. In particular, composite objects with $p = 1$ may become particularly stable, corresponding to a population ratio $n_2/n_1 = \kappa \in \mathbb{N}$; in such a situation, analogous to the above discussion of dimers, a term in $\mathcal{H}_b$ with the sine-Gordon-type form $G_{\kappa,1}\int dx \cos[2(\kappa\vartheta_1 - \vartheta_2)]$ may become relevant and stabilize a multimer liquid, uniquely identified by the finite gap associated with the bound-state formation and an algebraic decay of multimer correlations $\langle \mathcal{M}^\dagger(0)\mathcal{M}(x)\rangle$, $\mathcal{M} = (\psi_1)^\kappa \psi_2$, while the single-particle and dimer correlations $\mathcal{D}(x)$ decay exponentially. However, qualitative estimates (see [19]) indicate that comparatively large interaction strengths are needed in order to stabilize such a liquid, and the critical strength increases with increasing κ. Thus, below, we focus on $\kappa = 1$, and we investigate numerically the possibility to realize a trimer liquid (TL) by considering the anisotropic extended Hubbard model with both interaction and hopping asymmetry, quantified by the ratios d_2/d_1 and t_2/t_1.

To get guidance on possible trimer instabilities, we first compute the binding energy of the three-body problem: $\Delta_B = \lim_{L\to\infty}[E_L(1,1) + E_L(0,1) - E_L(1,2)]$. Based on a Born-Oppenheimer approach [23], we expect a sizable binding in the regime $t_1 \gg t_2$ and $d_1 \gtrsim d_2$, where a fast particle in wire 1 binds two repulsive heavy molecules in wire 2. Numerical examples of Δ_B vs t_2/t_1 are given in the inset in Fig. 3, for a few values of d_2, d_1, and $g = \lambda/2$, as trimers are unfavored for too large or too small interwire distances [19]. In particular, for strong attraction with $g \ll \lambda$, the formation of a dimer plus an unpaired particle is favored (see also the discussion of phase separation below). We have further investigated the phase diagram in the low-density limit ($n_2 = 2n_1 = 0.2$ and 0.1) as a function of d_1 and d_2 for system sizes up to $L = 120$ using the density-matrix-renormalization-group technique. The TL phase is characterized by an exponential decay of both $\mathcal{D}(x)$ and single-particle correlation function $\mathcal{C}_\alpha(x) = \langle c^\dagger_{\alpha,i} c_{\alpha,i+x}\rangle$, whereas the trimer correlator $\mathcal{T}(x) = \langle c^\dagger_{1,i} c^\dagger_{2,i} c^\dagger_{2,i+1} c_{2,i+x+1} c_{2,i+x} c_{1,i+x}\rangle$ decays algebraically. This is in contrast to the case of two coupled TLLs, where no correlation is exponentially suppressed. The phase diagram for $d_1 = 6d_2$, $n_2 = 0.1$ is plotted in Fig. 3 (see also [19] for the dependence on d_1/d_2): The TL extends in a broad region and survives even for comparatively small interaction strength and interaction asymmetry, albeit in both cases small hopping rates $t_2 \leq 0.2$ are needed. Sample correlation functions for both TL and 2TLL are plotted in Figs. 3(b) and 3(c). For large interactions $d_1 d_2/g^3 \gg t_\alpha$, *microscopic* phase separation can occur.

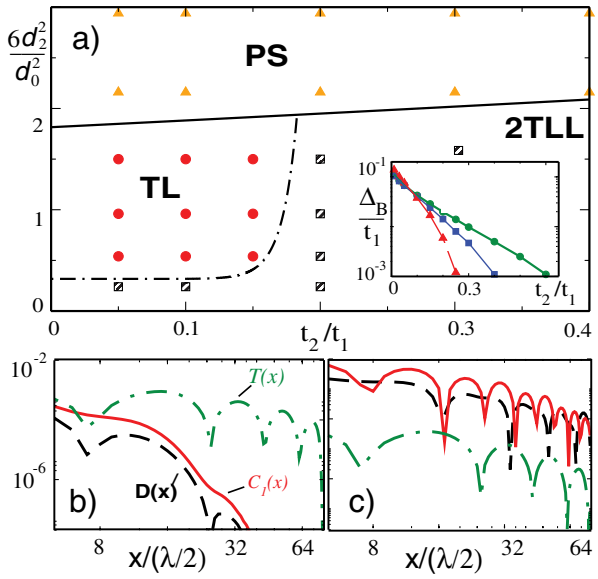

FIG. 3 (color online). (a) Phase diagram in the unbalanced case, as a function of d_1^2/d_0^2 and t_2/t_1. Here, $d_1 = 6d_2$, $g = \lambda/2$, $n_2 = 2n_1 = 0.1$, and $d_0^2 = t_1(\lambda/2)^3$; circles, triangles, and squares are numerical results for the TL, phase separation (PS), and two independent Tomonaga-Luttinger-liquid phases (2TLL), respectively; lines are guides for the eye. Inset: Trimer binding energy Δ_B/t_1 vs t_2/t_1 for several choices of $(d_1/d_0; d_2/d_0)$: triangles, squares, and circles are (0.5; 3), (0.3; 1.8), and (0.5, 2), respectively. (b)–(c) Correlation functions for trimers $\mathcal{T}(x)$ (dashed-dotted line), independent TLL $\mathcal{C}_1(x)$ (continuous line), and dimer liquid $\mathcal{D}(x)$ (dashed line) vs x in a system of size $L = 120$ (see the text). (b) Correlations in a TL with $d_1/d_0 = 3$, $d_2/d_0 = 0.5$, and $t_2/t_1 = 0.1$; (c) 2TLL with $d_1/d_0 = 2.4$, $d_2/d_0 = 0.4$, and $t_2/t_1 = 0.4$.

The latter corresponds to the formation of a gas of strongly bound, mutually repulsive dimers across the wires, coexisting with a gas of unpaired molecules in wire 2; see [19].

Effect of the trap.—We have investigated the fate of these exotic trimer bound states in the lattice under conditions of harmonic trapping in finite-size potentials with Hamiltonian $\hat{H}_t = (\mathcal{K}/L^2)\sum_i n_i(L/2 - i)^2$, with $\mathcal{K}$ the curvature. We characterize the TL phase in inhomogeneous trapped systems via the local order parameter $\delta n_i = 2n_{1,i} - n_{2,i}$, describing the deviations between the density of the majority and minority components [19]. Trimers exist if $\delta n_i \ll 1$. We find that trimers are remarkably robust to the presence of high-density, finite-size effects and fluctuations in particle numbers in the wires. The general situation is one where composite particles with a larger mass (e.g., trimers) occupy the central region of the trap and are flanked by lighter particles, being dimers or single excess particles. This determines an unusual "wedding-cake" structure in the density profile, reminiscent of that observed with a cold atom with contact interactions [15]. Figures 1(e) and 1(f) show example results of the density profile in the trap, in the presence of composite trimers for a case of an exactly matching number of particles in the two wires, and a situation where the particle number in wire 2 is larger by 20%. In both cases, we find a well-defined region at the trap center where trimers are formed, with $\delta n_i \sim 10^{-8}$.

Significant asymmetry in dipoles and mass is obtained in mixtures of, e.g., LiCs and RbCs molecules trapped in independent optical lattices, where a weak optical lattice in the wire direction provides additional tuning of the (effective) mass. Alternatively, single-species molecules can be prepared in different internal (e.g., rotational, vibrational) states with different dipole moments [8,24]. For a 1D lattice in the wire direction, the effective mass is tuned via internal-state-dependent tensor shifts [24,25]. All phases discussed above can be detected via the measurement of decay of correlation functions [see, e.g., Figs. 3(b) and 3(c)], using, e.g., direct *in situ* imaging techniques [26]. Particle correlations across the wires will be detected via *in situ* imaging [26] as well as noise correlation measurements [15]. In addition, the TL, DL, and DC may be spectroscopically probed [13]. For example, molecular dimers with sizable, spectroscopically resolvable gaps $\Delta_s \gtrsim 1$ μK are obtained by trapping, e.g., LiCs molecules in a deep 2D optical lattice with spacing $\lambda/2 = 400$ and trapping frequency $\omega_\perp = 2\pi \times 100$ kHz.

The realization of the above scenario in polar molecule experiments will lead to the first observation of trimers in the many-body context with cold gases.

We thank E. Burovski and A. Chotia for discussions and E. Ercolessi and F. Ortolani for discussions and for providing the density-matrix-renormalization-group code. This work was supported by MURI, AFOSR, EOARD, IQOQI, the Austrian FWF, the EU through NAME-QUAM, COHERENCE, and AQUTE.

Note added.—After completion of this work, we became aware of the related work [27] on few-body bound states of polar molecules in coupled tubes.

[1] R. Matsunaga, K. Matsuda, and Y. Kanemitsu, Phys. Rev. Lett. **106**, 037404 (2011).
[2] J. Sudan, A. Luscher, and A. M. Lauchli, Phys. Rev. B **80**, 140402(R) (2009).
[3] *Ultracold Fermi Gases*, edited by M. Inguscio, W. Ketterle, and C. Salomon (IOS, Amsterdam, 2008).
[4] P. Fulde and R. A. Ferrell, Phys. Rev. **135**, A550 (1964); A. I. Larkin and Yu. N. Ovchinnikov, Zh. Eksp. Teor. Fiz. **47**, 1136 (1964).
[5] G. Sarma, J. Phys. Chem. Solids **24**, 1029 (1963).
[6] F. Ferlaino and R. Grimm, Physics **3**, 9 (2010).
[7] H. P. Büchler *et al.*, Phys. Rev. Lett. **98**, 060404 (2007); A. Micheli *et al.*, *ibid.* **105**, 073202 (2010); G. Quéméner and J. L. Bohn, Phys. Rev. A **81**, 022702(R) (2010).
[8] M. H. G. de Miranda *et al.*, Nature Phys. **7**, 502 (2011).
[9] D. Wang *et al.*, Phys. Rev. Lett. **93**, 243005 (2004); J. M. Sage *et al.*, *ibid.* **94**, 203001 (2005); T. Rieger *et al.*, *ibid.* **95**, 173002 (2005); J. Deiglmayr *et al.*, *ibid.* **101**, 133004

(2008); S. D. Kraft *et al.*, J. Phys. B **39**, S993 (2006); S. Y. T. van de Meerakker *et al.*, Nature Phys. **4**, 595 (2008); J. Deiglmayr *et al.*, Phys. Rev. A **82**, 032503 (2010); A. D. Lercher *et al.*, arXiv:1101.1409 [Eur. Phys. J. D (to be published)].

[10] D.-W. Wang, M. D. Lukin, and E. Demler, Phys. Rev. Lett. **97**, 180413 (2006).

[11] C. Kollath, J. S. Meyer, and T. Giamarchi, Phys. Rev. Lett. **100**, 130403 (2008); A. Argüelles and L. Santos, Phys. Rev. A **75**, 053613 (2007); C.-M. Chang *et al.*, *ibid.* **79**, 053630 (2009).

[12] A. Pikovski *et al.*, Phys. Rev. Lett. **105**, 215302 (2010); A. C. Potter *et al.*, *ibid.* **105**, 220406 (2010); M. Baranov *et al.*, Phys. Rev. A **83**, 043602 (2011); R. M. Lutchyn, E. Rossi, and S. Das Sarma, *ibid.* **82**, 061604(R) (2010).

[13] E. Burovski, G. Orso, and T. Jolicoeur, Phys. Rev. Lett. **103**, 215301 (2009); G. Orso, E. Burovski, and T. Jolicoeur, *ibid.* **104**, 065301 (2010); G. Roux, E. Burovski, and T. Jolicoeur, Phys. Rev. A **83**, 053618 (2011).

[14] M. Dalmonte, G. Pupillo, and P. Zoller, Phys. Rev. Lett. **105**, 140401 (2010).

[15] I. Bloch, J. Dalibard, and W. Zwerger, Rev. Mod. Phys. **80**, 885 (2008).

[16] Coupled 1D wires can be obtained, e.g., by selective evaporation using (electric) field gradients, analogous to [28]. Amodsen Chotia (private communications).

[17] S. A. Meek *et al.*, Phys. Rev. A **83**, 033413 (2011); S. A. Meek *et al.*, Science **324**, 1699 (2009).

[18] T. Giamarchi, *Quantum Physics in One Dimension* (Oxford University, New York, 2003).

[19] See Supplemental Material at http://link.aps.org/supplemental/10.1103/PhysRevLett.107.163202 for further details.

[20] E. Haller *et al.*, Nature (London) **466**, 597 (2010).

[21] T. Lahaye *et al.*, Rep. Prog. Phys. **72**, 126401 (2009).

[22] U. Schollwöck, Rev. Mod. Phys. **77**, 259 (2005).

[23] D. S. Petrov *et al.*, Phys. Rev. Lett. **99**, 130407 (2007).

[24] A. Micheli *et al.*, Phys. Rev. A **76**, 043604 (2007).

[25] B. Friedrich and D. Herschbach, Phys. Rev. Lett. **74**, 4623 (1995); S. Kotochigova and E. Tiesinga, Phys. Rev. A **73**, 041405(R) (2006).

[26] C. Weitenberg *et al.*, Nature (London) **471**, 319 (2011); J. Simon *et al.*, *ibid.* **472**, 307 (2011).

[27] B. Wunsch *et al.*, Phys. Rev. Lett. **107**, 073201 (2011).

[28] S. Stock *et al.*, Phys. Rev. Lett. **95**, 190403 (2005).